A porous composite film synthesized by the disproportionation of a copper(I) complex at the toluene/water interface

Kun Luo and Robert A. W. Dryfe*

Received (in Cambridge, UK) 28th March 2007, Accepted 4th May 2007
First published as an Advance Article on the web 31st May 2007
DOI: 10.1039/b704638c

Porous copper/copper oxide films form *via* spontaneous reduction at the liquid/liquid interface.

The liquid/liquid interface offers potential as an environment to assemble nanoparticles (NPs) into films, since the particles are highly mobile and easily reach an equilibrium on self-assembly at the interface.[1–4] Another route to create ordered monolayers at liquid/liquid interfaces is *via* interfacial reaction. Rao *et al.*[5–9] recently reported that a series of ultrathin films have been prepared by interfacial reduction at the toluene/water interface, which has attracted particular interest as a simple route to the preparation of ultrathin "essentially defect free" films.[7] Within the series, Cu nanocrystalline films[9] with some oxide impurity were prepared by the interfacial reaction between chloro(triphenylphosphine) copper ($Cu(PPh_3)Cl$) in toluene and aqueous phase sodium hydroxide, without introducing any other reducing agents. No mechanism was proposed to explain how the Cu(I) complex was reduced to Cu. It is also reported that the composition of the interfacial deposit is dependent on the concentration of hydroxide ions as copper acetylacetonate ($Cu(cup)_2$, a planar Cu(II) complex[10]) in toluene reacts with NaOH,[7] where CuO films were obtained when the hydroxide concentration exceeded 0.75 M, and $Cu(OH)_2$ nanocrystals were prepared when 0.1 M NaOH solution was used. Saravanan *et al.* obtained CuO "nanowhiskers" *via* a similar route.[11] Planar metal complexes have been used to prepare one-dimensional (1D) nanostructures at the liquid/liquid interface since growth is believed to occur preferentially along the vertical direction to form nanorods, due to the steric inhibition on the planes.[12,13] Song *et al.*[14] employed a square-planar molecule, bis(ethylhexyl)hydrogen phosphate copper ($Cu(DEHP)_2$), to synthesize $Cu(OH)_2$ nanowires. Electrochemical deposition of copper at the liquid/liquid interface has been reported, using an organic phase electron donor.[15] Herein, we present recent results that chlorotris(triphenylphosphine) copper(I) ($Cu(PPh_3)_3Cl$) with tetrahedral coordination geometry[16] reacts with NaOH solution at the toluene/water interface, and both ultrathin copper films and copper oxide/hydroxide nanofibres can be obtained simultaneously in a composite porous film.

Typically, a solution of $Cu(PPh_3)_3Cl$ in toluene was added to a glass tube containing an aqueous solution of NaOH and allowed to react at ambient temperature (see Experimental† for typical concentrations). A thin film appeared at the toluene/water interface after 4.5 hours of contact time with high coverage rate, and after 24 hours the film became thicker and rougher with some cracks apparent under the optical microscope at 160-fold magnification (not shown), which also suggests that the film is somewhat brittle. The scanning electron micrograph of the film after 24 hour reaction displays a porous structure (see Fig. 1), with the average diameter of the pores determined from the image being around 0.8 μm. The framework is actually composed of bundles of fibres, with an ultrathin film that encapsulates the fibres, extending to cover part of the pores as well, which finally leads to a unique semi-closed porous film (see Fig. 1a and b). The distribution of the fibres in diameter is quite uniform, which is suggestive of a templating aspect to the growth. The X-ray mapping analysis of the scanning electron micrograph illustrates that the elemental copper distribution is less closely bound to the structure of the ultrathin film (as shown in Fig. 1d), whereas the oxygen builds up the distinct framework in accord with Fig. 1a (shown in Fig. 1c). The oxygen-rich framework suggests that the fibres are probably composed of copper oxide or copper hydroxide. Correspondingly, the ultrathin film is elemental copper due to the distribution of copper in the pore area as background.

Further TEM investigation on the fibre separated from the framework is illustrated in Fig. 2. The HRTEM image in the inset of Fig. 2a illustrates that a crystalline zone exists with a lattice spacing of about 0.25 nm along with other amorphous regions in the fibre. The lattice spacing suggests the existence of monoclinic CuO crystals ($C2/c$, a = 4.684 Å, b = 3.425 Å, c = 5.129 Å, JCPDF No. 05-0661). The darkness in the middle of the fibre in Fig. 2a

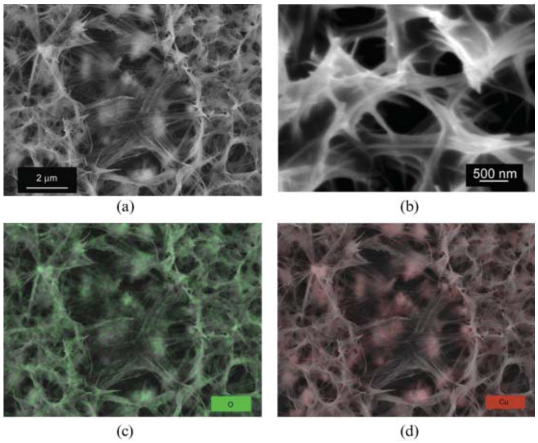

Fig. 1 The morphology and X-ray mapping analysis of the porous film formed at the water/toluene interface using the standard conditions given in the Experimental section. (a) SEM micrograph of the deposit; (b) detailed microstructure in higher magnification; (c) distribution of oxygen in the selected area; (d) distribution of copper in the selected area.

School of Chemistry, University of Manchester, Oxford Road, Manchester, UK M13 9PL. E-mail: robert.dryfe@manchester.ac.uk; Fax: +44 161 275 4734

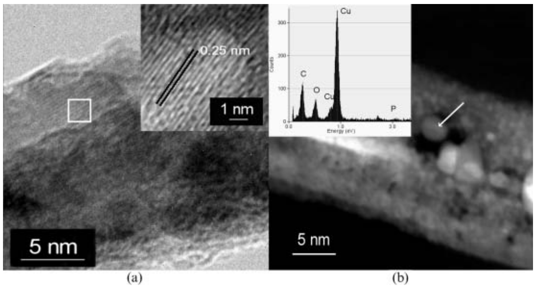

(a) (b)

Fig. 2 Transmission electron microscopy analysis of the fibre inside the framework of the interfacial deposit. (a) TEM image of the separated fibre, inset is the HRTEM of the selected region in the fibre; (b) STEM micrograph of the fibre, inset is the EDX result of the highlighted area.

suggests a cylindrical geometry, with a diameter of *ca.* 20 nm. This is confirmed by the STEM micrograph of the fibre (see Fig. 2b), and the EDX analysis shows that copper is uniformly present in the fibre, but oxides or hydroxides are irregularly distributed. The Cu particle (the bright particle in Fig. 2b) was observed and the related EDX result is shown as well. Hence, the porous film is actually a combination of copper film and copper oxide/hydroxide fibres.

The XRD analysis in Fig. 3 shows a complex pattern obtained for the film after 24 hour reaction at the toluene/water interface. The strong diffraction peaks of (200), (220), (311) and (400) are assigned as Cu (JCPDF No. 02-1225, corresponding lattice spacings are 1.810, 1.280, 1.090 and 0.900 Å). The other strong patterns corresponding to the diffraction of ($\bar{1}$11), ($\bar{1}$13), (220) and ($\bar{4}$22) are attributed to CuO (JCPDF No. 05-0661, corresponding lattice spacings are 2.523, 1.505, 1.375 and 0.939 Å), which is in accord with the EDX analysis. The diffraction peaks at low angles possibly correspond to the diffraction peaks of (002) and (012) of $Cu(OH)_2$ hydrate, respectively (JCPDF No. 42-0638, corresponding lattice spacings are 3.312 Å and 2.516 Å).

The coexistence of Cu, CuO and $Cu(OH)_2$ after the interfacial reaction between the copper(I) complex in toluene and the NaOH solution can be understood as disproportionation, due to the following relevant standard potentials, relative to the hydrogen electrode:[17]

$$Cu^{2+} \xleftarrow{-0.153\ V} Cu^{+} \xrightarrow{0.521\ V} Cu^{0} \tag{1}$$

which finally leads to copper and copper oxide (CuO)/hydroxide ($Cu(OH)_2$) in a basic solution, and the proposed interfacial reactions are described as follows:

$$Cu(PPh_3)_3Cl_{(org)} + NaOH_{(aq)} \rightarrow Cu(OH)_{(\sigma)} + 3PPh_{3(org)} + NaCl_{(aq)} \tag{2}$$

$$2Cu(OH)_{(\sigma)} \rightarrow Cu_2O_{(\sigma)} + H_2O_{(aq)} \tag{3}$$

$$Cu_2O_{(\sigma)} \rightarrow CuO_{(\sigma)} + Cu_{(\sigma)} \tag{4}$$

$$Cu_2O_{(\sigma)} + H_2O_{(aq)} \rightarrow Cu(OH)_{2(\sigma)} + Cu_{(\sigma)} \tag{5}$$

The subscripts "σ", "aq", and "org" in the equations represent interfacial, aqueous and organic phases, respectively. The Cu(OH) intermediate is formed from ligand exchange between PPh_3 and OH^-. The unstable cuprous hydroxide is in turn transformed into Cu_2O,[18] which disproportionates to Cu and CuO or $Cu(OH)_2$, as shown in eqn (4) and (5). The low solubility of Cu_2O, $Cu(OH)_2$ and CuO[19] shifts the equilibrium of eqn (1) to the products, and allows the reaction to be completed. CuO could be prepared instead of $Cu(OH)_2$ with sufficient NaOH.[11] However, in the case of low OH^- concentration, a mixture of Cu, $Cu(OH)_2$ and CuO is probably obtained. The concentration of NaOH in the present experiment was marginally higher than that used to form a Cu monolayer.[9] According to the above reactions, the mixture of Cu, $Cu(OH)_2$ and CuO should be obtained firstly at the interface since the concentration of OH^- is relatively high. As the content of OH^- ions drops, Cu film forms and finally covers the mixture.

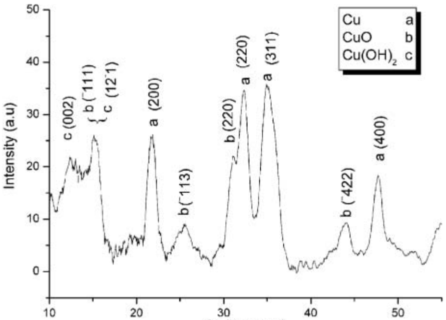

Fig. 3 X-Ray diffraction pattern of the interfacial deposit (see inset for key).

The experiment shows the availability of both Cu ultrathin film and copper oxide/hydroxide nanofibres by interfacial disproportionation, although a tetrahedrally coordinated $Cu(PPh_3)_3Cl$ molecule was employed instead of the linear copper(I) complex ($Cu(PPh_3)Cl$) for a Cu nanocrystalline film[9] and the planar copper(II) complexes for copper oxide/hydroxide nanofibres.[11,14] Fig. 4 displays the SEM images for the interfacial deposits under different conditions. The product obtained at 50 °C with the standard content in both phases (Fig. 4a, see Experimental†) shows that the fibres became broader and the films grew thick. When a high concentration of NaOH (0.75 M) was used in the

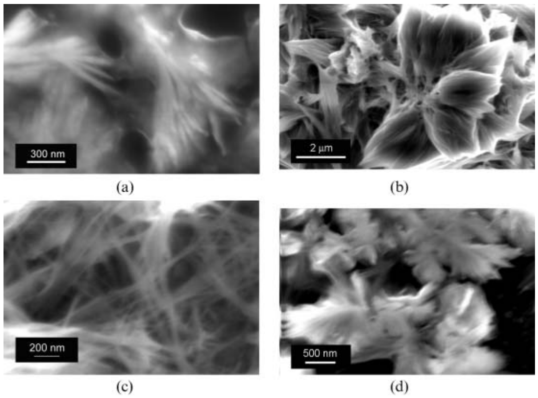

(a) (b)

(c) (d)

Fig. 4 SEM images of the interfacial deposits under different conditions. (a) 5 ml of 1.5 mM $Cu(PPh_3)_3Cl$ in toluene reacted with 8 ml of 20 mM NaOH water solution at 50 °C; (b) as a, but the NaOH concentration was increased to 0.75 M and deposition occurred at room temperature; (c) 5 ml of saturated $Cu(PPh_3)_3Cl$ in toluene reacted with 8 ml of 20 mM NaOH aqueous solution in room temperature; (d) as c, but the $Cu(PPh_3)_3Cl$ concentration was reduced to 0.6 mM.

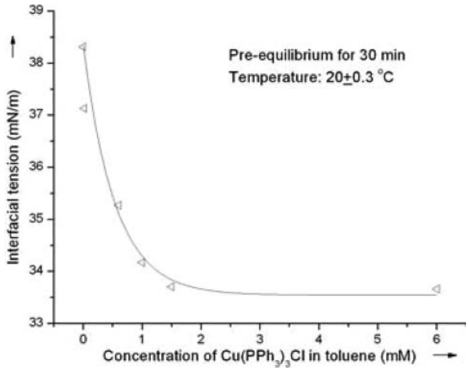

Fig. 5 Interfacial tension measurement at the toluene/water interface as a function of the concentration of $Cu(PPh_3)_3Cl$ in toluene.

aqueous phase, the fibres merged into thick layers of the deposit, which resemble "flowers" (see Fig. 4b). If the concentration of $Cu(PPh_3)_3Cl$ in the toluene phase is increased to saturation, the SEM micrograph of Fig. 4c presents a more fibrous appearance, and it is hard to find any thin films. When a lower concentration of $Cu(PPh_3)_3Cl$ (0.6 mM) was used, a discontinuous interfacial deposit was yielded with the fibres staying with the films. The common feature for all the observations of the interfacial deposits is the large number of coagulated particles in the centre, from where fibres and thin layers extend, suggesting the fibres and films were formed after the initial nucleation due to the increasing rate of growth. Higher concentrations of $Cu(PPh_3)_3Cl$ form more fibres, while higher reaction rates (high NaOH concentration or higher temperatures) tend to produce thicker films. However, although the mechanism of nanofibre formation from the tetrahedrally coordinated Cu(I) complex is unclear, one plausible factor is the surface activity of the Cu(I) complex. Fig. 5 shows that the interfacial tension of the toluene/water interface decreases as the $Cu(PPh_3)_3Cl$ concentration in toluene is increased. The amphiphilic nature of this species is likely to influence deposit morphology. The CuO and $Cu(OH)_2$ products are likely to grow in an anisotropic fashion under kinetic control,[20] given their respective monoclinic and triclinic structures, favouring the formation of interfacial fibres. The cubic copper structure, by contrast, will favour film formation at the interface. The importance of amphiphiles in interfacial deposition processes has been noted previously.[21]

In summary, the interfacial disproportionation of copper(I) complex allows the low-cost and facile preparation of a porous film with both Cu films and $CuO/Cu(OH)_2$ nanofibres. This experiment also indicates that the possible self-assembly of tetrahedrally coordinated $Cu(PPh_3)_3Cl$ molecules at the toluene/water interface induces a template-assisted synthesis of cupric oxide/hydroxide nanofibres, which highlights the importance of amphiphilic precursor molecules in deposition at the liquid/liquid interface: this aspect has not been reported previously to our knowledge. The magnetic properties of $Cu(OH)_2$ are sensitive to the intercalation of anions, making the material a candidate for sensor applications.[14] Cu[22] and CuO[14] are used as heterogeneous catalysts, hence their combination into a porous film is of interest in catalyst and/or sensor design.

The authors thank the UK Engineering & Physical Science Research Council for financial support (EP/C509773/1).

Notes and references

† *Experimental*: Analytical grade chlorotris(triphenylphosphine) copper(I) ($Cu(PPh_3)_3Cl$, Aldrich) and sodium hydroxide (NaOH, Aldrich) were used directly without further treatment. Pure water (18.2 MΩ cm) was obtained from an Elga "Purelab Ultra" (Elga, Marlow, UK) system. A 5 ml solution of 1.5 mM $Cu(PPh_3)_3Cl$ in toluene was added to a glass tube containing 8 ml of an aqueous solution composed of 20 mM sodium hydroxide (NaOH); the mixture was kept at ambient temperature for 24 hours. The tube, which was of 25 mm diameter and 75 mm high, was closed with a cap. A digital camera was used to record the formation of the film at the toluene/water interface. The *in-situ* observation of the interfacial reaction was performed using a Leica DMIL optical microscope fitted with a Sony CCD-IRIS camera at 160-fold magnification. The interfacial deposits were transferred onto glass slides and dried in air, and were washed with pure water and acetone and dried at ambient temperature before further analysis. The X-ray diffraction (XRD) analysis was carried out by an Oxford Diffraction System (Xcalibur 2, Mo $K\alpha = 0.7093$ Å), and an XL 30 FEG Philips electron microscope was employed at 10 kV for scanning electron microscopy (SEM) and at 20 kV for X-ray mapping analysis. Transmission electron microscopy (TEM), high resolution transmission microscopy (HRTEM), scanning transmission microscopy (STEM) and energy dispersive X-ray (EDX) analysis were performed with a Tecnai F30 FEG-TEM system operating at 300 kV. The interfacial tension measurement was accomplished using a Kruss Processor Tensiometer K12 (V3.46), and related density measurements were completed by using a DMA 45 Calculating Digital Density Meter (AP PAAR): both operations were conducted at 20 ± 0.3 °C.

1 D. Y. Wang, H. W. Duan and H. Möhwald, *Soft Matter*, 2005, **1**, 412–416.
2 W. H. Binder, *Angew. Chem., Int. Ed.*, 2005, **44**, 5172–5175.
3 J. K. Sakata, A. D. Dwoskin, J. L. Vigorita and E. M. Spain, *J. Phys. Chem. B*, 2005, **109**, 138–141.
4 T. Maddanimath, A. Kumar, J. D'Arcy-Gall, P. G. Ganesan, K. Vijayamohanan and G. Ramanath, *Chem. Commun.*, 2005, 1435–1437.
5 V. V. Agrawal, G. U. Kulkarni and C. N. R. Rao, *J. Phys. Chem. B*, 2005, **109**, 7300–7305.
6 V. V. Agrawal, P. Mahalakshmi, G. U. Kulkarni and C. N. R. Rao, *Langmuir*, 2006, **22**, 1846–1851.
7 U. K. Gautam, M. Ghosh and C. N. R. Rao, *Langmuir*, 2004, **20**, 10775–10778.
8 C. N. R. Rao, G. U. Kulkarni, V. V. Agrawal, U. K. Gautam, M. Ghosh and U. Tumkurkar, *J. Colloid Interface Sci.*, 2005, **289**, 305–318.
9 C. N. R. Rao, G. U. Kulkarni, P. J. Thomas, V. V. Agrawal and P. Saravanan, *J. Phys. Chem. B*, 2003, **107**, 7391–7395.
10 Y. Elerman, O. Atakol, I. Svoboda and M. Geselle, *Acta Crystallogr., Sect. C: Cryst. Struct. Commun.*, 1995, **51**, 1520–1522.
11 P. Saravanan, S. Alam and G. N. Mathur, *Thin Solid Films*, 2005, **491**, 168–172.
12 Y. J. Xiong, Y. Xie, G. O. Du, X. M. Liu and X. B. Tian, *Chem. Lett.*, 2002, **1**, 98–99.
13 Y. D. Li, M. Sui, Y. Ding, G. H. Zhang, J. Zhuang and C. Wang, *Adv. Mater.*, 2000, **12**, 818–821.
14 X. Y. Song, S. X. Sun, W. M. Zhang, H. Y. Yu and W. L. Fan, *J. Phys. Chem. B*, 2004, **108**, 5200–5205.
15 M. Guainazzi, G. Silvestri and G. Serravalle, *J. Chem. Soc., Chem. Commun.*, 1975, 200–201.
16 T. F. Carlson, Jr., J. P. Fackler and R. A. Kresinski, *Acta Crystallogr., Sect. C: Cryst. Struct. Commun.*, 1996, **C52**, 1117–1119.
17 P. Vanýsek, in *CRC Handbook of Chemistry and Physics*, ed. R. D. Lide and H. P. R. Frederikse, CRC Press, Boca Raton, USA, 76th edn, 1995, pp. 8–22.
18 M. Pourbaix, in *Atlas of Electrochemical Equilibria in Aqueous solutions*, Pergamon, Oxford, UK, 2nd edn, 1974, ch. IV, p. 388.
19 W. Feitknecht, *Helv. Chim. Acta*, 1944, **27**, 771–775.
20 S. M. Lee, S. N. Cho and J. Cheon, *Adv. Mater.*, 2003, **15**, 441–444.
21 D. Yogev and S. Efrima, *J. Phys. Chem.*, 1988, **92**, 5754–5760.
22 H. Bluhm, M. Hävecker, A. Knop-Gericke, E. Kleimenov and R. Schlögl, *J. Phys. Chem. B*, 2004, **108**, 14340–14347.